

# A Statistical Approach to WindSat Ocean Surface Wind Vector Retrieval

Craig K. Smith, *Member, IEEE*, Michael Bettenhausen, *Member, IEEE*, and Peter W. Gaiser, *Senior Member, IEEE*

**Abstract**—WindSat is the first space-based polarimetric microwave radiometer. It is designed to evaluate the capability of polarimetric microwave radiometry to measure ocean surface wind vectors from space. The sensor provides risk reduction for the National Polar-orbiting Operational Environmental Satellite System Conical Scanning Microwave Imager/Sounder, which is planned to provide wind vector data operationally starting in 2010. The channel set also enables retrieval of sea surface temperature, and columnar water vapor and cloud liquid water over the oceans. We describe statistical algorithms for retrieval of these parameters, and a combined statistical/maximum-likelihood estimator algorithm for retrieval of wind vectors. We present a quantitative analysis of the initial wind vector retrievals relative to QuikSCAT wind vectors.

**Index Terms**—Microwave radiometry, polarimetry, retrievals, wind.

## I. INTRODUCTION

WINDSAT is a conically scanning polar-orbiting multi-frequency microwave radiometer launched in January 2003. Its objective is to measure the partially polarized emission from the ocean surface and, therefore, test and fully evaluate the viability of using polarimetric microwave radiometry to retrieve ocean surface wind vectors. WindSat measures polarized radiometric brightness temperatures ( $T_B$ ) in 16 “channels”: vertically and horizontally polarized  $T_B$  ( $T_V$  and  $T_H$ ) at 6.8, 10.7, 18.7, 23.8, and 37.0 GHz, and third and fourth Stokes parameters ( $T_U$  and  $T_4$ ) at 10.7, 18.7, and 37.0 GHz.  $T_U$  and  $T_4$  are derived from the difference of  $\pm 45^\circ$  linear and left/right circular polarizations, respectively. The WindSat reflector antenna has an 11-feedhorn cluster, resulting in fixed nominal Earth incidence angles (EIA) ranging from  $50^\circ$  to  $56^\circ$  (all horns within a frequency band have the same EIA) [1]. The EIAs are known to better than  $0.05^\circ$  [2]. A detailed description of the radiometer can be found in [1]. WindSat provides risk reduction for the Conically Scanning Microwave Imager/Sounder to be flown on the National Polar-orbiting Operational Environmental Satellite System [3].

We have developed an empirical statistical regression technique for retrieval of sea surface temperature (SST), wind speed

TABLE I  
NOMINAL NEDT VALUES FOR RAIN-FREE OCEAN RETRIEVAL CELLS (IN KELVIN)

	6.8	10.7	18.7	23.8	37.0
$T_V, T_H$	0.111	0.036	0.033	0.063	0.023
$T_U, T_4$	-	0.053	0.049	-	0.036

(W) referenced to 10-m height, compass wind direction ( $\varphi$ ), columnar water vapor (V), and cloud liquid water (L). The purpose of this effort is threefold: 1) obtain a quick initial assessment of WindSat’s wind vector measurement capabilities; 2) provide a retrieval-oriented test platform for enhancements to the WindSat Temperature and Sensor Data Record algorithms; and 3) provide either an independent set of retrievals from, or *a priori* data for, a physically based algorithm. The regression technique and the selection of regression training data were designed to facilitate retrieval of all five parameters, as discussed in Sections II and V. However, in this letter we focus on application of the regressions to wind vector retrieval.

## II. REGRESSION TECHNIQUE

For this initial validation of the regression technique, we used WindSat  $T_B$  averaged to the lowest resolution (6.8 GHz), where the  $T_B$  for all 16 channels are available. The  $T_B$  for each channel are sampled at approximately 12.5 km along scan and along track and averaged to a common spatial resolution of approximately  $40 \times 60$  km. The nominal measurement noise for the retrieval cells, specified by the noise-equivalent differential temperature (NEDT) for mean ocean scene  $T_B$ , is given in Table I.

The regression training (i.e., regression coefficient determination) is performed empirically, using collocations of WindSat  $T_B$  with various sources of satellite retrievals and numerical weather prediction model (NWP) data (Section V). Unlike regressions trained using  $T_B$  simulated with a physical model [4], [5], empirical regressions automatically compensate for bias errors in the measurements, and potential problems such as time-dependent calibration errors or high noise results in deemphasis (coefficients near zero) for the affected channel. Therefore, we use all 16 channels in all regressions. Regression coefficients are determined by linear least squares.

We use a linear method to retrieve parameters for which the relationship with the  $T_B$  ranges from nearly linear to severely nonlinear. Three techniques exist to address this nonlinearity problem. The first uses functions of the  $T_B$  that are linear with respect to a given retrieval parameter as arguments in the regressions [4], [5]. Additionally, terms that are quadratic or higher order in the  $T_B$  or the linearization functions may be included

Manuscript received December 21, 2004; revised August 5, 2005. This work was supported in part by the U.S. Navy under Grant N000WX04730023.

C. K. Smith was with Computational Physics, Inc., Springfield, VA 22151 USA. He is now with The Aerospace Corporation, Los Angeles, CA 90009 USA.

M. Bettenhausen and P. W. Gaiser are with the Remote Sensing Division, Naval Research Laboratory, Washington DC, 20375 USA (e-mail: peter.gaiser@nrl.navy.mil).

Digital Object Identifier 10.1109/LGRS.2005.860661

# Report Documentation Page

Form Approved  
OMB No. 0704-0188

Public reporting burden for the collection of information is estimated to average 1 hour per response, including the time for reviewing instructions, searching existing data sources, gathering and maintaining the data needed, and completing and reviewing the collection of information. Send comments regarding this burden estimate or any other aspect of this collection of information, including suggestions for reducing this burden, to Washington Headquarters Services, Directorate for Information Operations and Reports, 1215 Jefferson Davis Highway, Suite 1204, Arlington VA 22202-4302. Respondents should be aware that notwithstanding any other provision of law, no person shall be subject to a penalty for failing to comply with a collection of information if it does not display a currently valid OMB control number.

1. REPORT DATE <b>JAN 2006</b>		2. REPORT TYPE		3. DATES COVERED <b>00-00-2006 to 00-00-2006</b>	
4. TITLE AND SUBTITLE <b>A Statistical Approach to WindSat Ocean Surface Wind Vector Retrieval</b>				5a. CONTRACT NUMBER	
				5b. GRANT NUMBER	
				5c. PROGRAM ELEMENT NUMBER	
6. AUTHOR(S)				5d. PROJECT NUMBER	
				5e. TASK NUMBER	
				5f. WORK UNIT NUMBER	
7. PERFORMING ORGANIZATION NAME(S) AND ADDRESS(ES) <b>Naval Research Laboratory, Remote Sensing Division, 4555 Overlook Avenue, SW, Washington, DC, 20375</b>				8. PERFORMING ORGANIZATION REPORT NUMBER	
9. SPONSORING/MONITORING AGENCY NAME(S) AND ADDRESS(ES)				10. SPONSOR/MONITOR'S ACRONYM(S)	
				11. SPONSOR/MONITOR'S REPORT NUMBER(S)	
12. DISTRIBUTION/AVAILABILITY STATEMENT <b>Approved for public release; distribution unlimited</b>					
13. SUPPLEMENTARY NOTES <b>The original document contains color images.</b>					
14. ABSTRACT					
15. SUBJECT TERMS					
16. SECURITY CLASSIFICATION OF:			17. LIMITATION OF ABSTRACT	18. NUMBER OF PAGES <b>5</b>	19a. NAME OF RESPONSIBLE PERSON
a. REPORT <b>unclassified</b>	b. ABSTRACT <b>unclassified</b>	c. THIS PAGE <b>unclassified</b>			

to allow the regression training to eliminate some of the nonlinearity directly [5]. The second technique is to retrieve a function of the desired parameter, on which the  $T_B$  have an approximately linear dependence [5]. The third method is to train and apply regressions on restricted domains (“bins”) of a geophysical parameter on which the  $T_B$  have a nonlinear dependence. The bins are chosen so that the dependence of the  $T_B$  on that parameter is approximately linear within each bin [4].

The application of these techniques to the retrievals is explained below. We make a significant extension to the second technique to retrieve wind direction, for which the signal in all the  $T_B$  is severely nonlinear (in fact nonunique) and depends on wind speed. There, we perform regressions for several functions of wind speed and direction, and then use the regression results in a maximum-likelihood estimator (MLE) for wind direction retrieval, as discussed in Section III.

The regression for any retrieval parameter  $P$  is of the form

$$P = a_0 + \sum_{i=1}^{16} a_i t_i + \sum_{i=1}^{16} b_i t_i^2 + c_1 e + c_2 e^2 \quad (1)$$

where  $t_i$  is the WindSat brightness temperature for channel  $i$  ( $T_{Bi}$ ), except for the 23.8-GHz channels, where  $t_i = \ln(290 - T_{Bi})$ ; the latter serves to linearize  $t_i$  with respect to the V signal when water vapor absorption is appreciable [4], [5], which significantly improves the V retrieval but does not significantly affect any of the other retrievals. The quadratic terms greatly reduce the nonlinear interactions (“crosstalk”) between SST, W, V, and L. Inclusion of the EIA for the 37-GHz vertical–horizontal (vh) feedhorn (e) reduces the SST retrieval error by 5%, but has little effect on the other retrievals. The small variations from the nominal EIAs for the different feedhorns show a linear relationship to each other, so that inclusion of a single EIA is sufficient for a linear regression. The regressions allow for direct retrieval of SST, W, V, and L.

The directional component of the microwave sea surface emissivity ( $\epsilon_{\text{dir}}$ ) can be expressed as a two-term Fourier series in relative wind direction ( $\varphi_R$ , the compass wind direction minus radiometer look direction projected on the Earth) [6]. The Fourier coefficients are nonlinear functions of wind speed that depend on Earth incidence angle, frequency, and polarization [6]. The series is even for  $T_v$  and  $T_h$  and odd for  $T_U$  and  $T_4$  [6], [7]

$$\begin{aligned} \epsilon_{\text{dir}} &= f_1(W) \cos \varphi_R + f_2(W) \cos 2\varphi_R; (T_v, T_h) \\ \epsilon_{\text{dir}} &= g_1(W) \sin \varphi_R + g_2(W) \sin 2\varphi_R; (T_U, T_4). \end{aligned} \quad (2)$$

Thus, for  $\varphi$  retrieval, we perform four regressions, for the along-look wind speed ( $U_1 = W \cos \varphi_R$ ), cross-look wind speed ( $U_2 = W \sin \varphi_R$ ), and “second harmonics” of the along- and cross-look wind speeds ( $U_3 = W \cos 2\varphi_R$  and  $U_4 = W \sin 2\varphi_R$ ). The along-look wind speed is identical to the “line-of-sight” wind speed retrieved by Wentz [8]. While the  $U_1$  and  $U_2$  regressions are sufficient for unique wind direction retrieval, we find significant improvement for  $W > 9$  m/s by using all four regressions as input to an MLE for wind direction retrieval.

The regressions are accomplished using a two-stage technique. In the first stage, the retrievals are performed for  $W$ ,  $V$ , and  $L$ , using regression coefficients trained on the entire training dataset (Section V). In the second stage, the first-stage  $W$  regression result is used to determine a wind speed bin, from which regression coefficients are selected to perform the SST and  $U_1$  through  $U_4$  retrievals. The bins are 2 m/s wide, and cover the wind speed ranges 0–2, 2–4, 4–6 m/s, etc.

The second-stage regressions offer significant advantages over analogous first-stage regressions. Within each bin the Fourier coefficients in (2) are approximately linear functions of  $W$ —i.e., the wind direction signals are approximately linear in  $U_1$  through  $U_4$ —improving the  $U_1$  through  $U_4$  linear regression and MLE wind direction performance.

Second-stage performance is improved by widening the bins during regression training, to account for the “misbinning” resulting from retrieval error in the first-stage  $W$  regression [0.8 m/s root mean square (rms) error]. However, the benefit of accommodating misbinning is counterbalanced by the increasing nonlinearity of the  $T_B$  with respect to  $U_1$  through  $U_4$  as the bins are widened. Given the bin width of 2 m/s for the retrievals, a bin width of 4 m/s for the training is optimal; the bins are thus widened by 1.0 m/s on each side for second-stage training (0–3, 1–5, 3–7 m/s, etc.).

### III. MAXIMUM-LIKELIHOOD ESTIMATOR

Following application of the second-stage regressions,  $U_1$  through  $U_4$  are provided to the MLE for wind direction retrieval. The likelihood function to be maximized is for estimating two parameters ( $W, \varphi_R$ ) from four “measurements” ( $U_1$  through  $U_4$ ) whose errors are correlated and approximately Gaussian distributed [9]. Therefore, the MLE finds multiple wind vector solutions, ( $W, \varphi_R$ ) pairs known as “ambiguities,” as local minima of

$$\chi^2 = \delta \vec{U}^T \cdot \mathbf{C}_U^{-1} \cdot \delta \vec{U}$$

where

$$\delta \vec{U} = \begin{pmatrix} U_1 - W \cos \varphi_R \\ U_2 - W \sin \varphi_R \\ U_3 - W \cos 2\varphi_R \\ U_4 - W \sin 2\varphi_R \end{pmatrix}.$$

$\mathbf{C}_U$  is the error covariance matrix of the  $U_1$  through  $U_4$  retrievals for the bin determined by the first-stage  $W$  regression (Section II) and is obtained by running the regressions on the training dataset (Section V). The  $\delta U$  vector is simply the difference between the  $U_1$  through  $U_4$  regressions and their mathematical definitions given in Section II.

The MLE may appear to be a two-dimensional search for chi-square minima in the space of ( $W, \varphi_R$ ). However, it should be noted that, because  $U_1$  through  $U_4$  are linear in  $W$ , minimization along the  $W$  axis yields a single, analytical solution for  $W$  at each value of  $\varphi_R$ , denoted  $W_{\min}(\varphi_R)$ . Substitution of  $W_{\min}(\varphi_R)$  into the definition of the chi-square results in a one-dimensional minimization along the  $\varphi_R$  axis. This one-dimensional minimization is subject to the following conditions: 1)  $W_{\min}(\varphi_R)$  is nonnegative (physical solution); 2) the second

partial derivative of the chi-square with respect to  $W$ , evaluated at  $W_{\min}(\varphi_R)$ , is positive (true minimum and not a saddle or inflection point).

The resulting  $(W_{\min}(\varphi_R), \varphi_R)$  ambiguities are then ranked by chi-square, with the “first rank” solution having the lowest chi-square. It should be noted that the  $U_1$  through  $U_4$  regressions have significantly larger retrieval errors than the first-stage  $W$  regression, and therefore the  $W_{\min}$ 's are inferior to the first-stage  $W$  regression result. We therefore use the first-stage  $W$  retrieval as the final retrieval result.

#### IV. MEDIAN FILTER

Due to regression errors, the first rank (most likely) solution is not always the closest ambiguity to the true wind direction. Improvement in ambiguity selection beyond the first rank result is made in retrieval postprocessing, where we apply a vector median filter (MF) [10] to correct isolated ambiguity selection errors while retaining the large scale discontinuities (for example, fronts) found in natural wind fields.

The MF is an iterative spatial filter that selects from the set of ambiguities in the cell being filtered the one most consistent with the previously selected ambiguities in a window of surrounding cells. It accomplishes this by minimizing the vector median filter function [10], a weighted sum of norms of vector differences between an ambiguity and the previously selected ambiguities for all cells in the window. After the MF is applied to all ocean cells in an orbit, the newly selected wind field replaces the previous wind field. The process is iterated until the wind field converges.

In our application, the window is  $7 \times 7$  cells (in scan-based coordinates) centered on and including the cell being filtered. Missing cells in the window (due to scan edges, land, ice, etc.), are “replaced” with the ambiguities from the center cell. Because wind direction retrieval performance improves with increasing  $W$  (Section VI), the term for each cell in the filter function is weighted linearly by the retrieved wind speed for that cell;  $\text{weight} = \min(0.1 * W, 1.0)$  for high confidence retrievals, and half that for low-confidence retrievals (Section V) and for replacements.

The MF is initialized with the first rank wind vector from each ocean retrieval cell. Optionally, it can be initialized with nudged wind vector fields [11]; the nudged field is obtained by selecting the first or second rank ambiguity for each cell that is closest to the wind vector obtained from the NCEP Global Data Assimilation System (GDAS)  $1^\circ \times 1^\circ$  analysis closest in time, spatially interpolated to the cell locations.

#### V. ALGORITHM TRAINING AND TESTING

Six months of WindSat version 1.6.1 Sensor Data Records (SDRs), spanning a period when thermal gradients in the warm load [12] are minimal (September 2003 through February 2004), have been collocated with various sources of NWP and satellite retrievals for use in regression training and retrieval testing (alternating two days training, one day testing throughout).

The training dataset consists of collocations between Windsat SDRs, the QuikSCAT science product [11] for wind vectors, and

SSM/I. GDAS  $1^\circ \times 1^\circ$  analyses spatially interpolated to the location of Windsat measurements are used for SST, and for wind vectors when a QuikSCAT observation is not available. The collocation with SSM/I is included to facilitate development of V and L regressions. The wind vector testing dataset is a two-way collocation between WindSat and QuikSCAT. For both training and testing, the spatial collocation window is 25 km for all data sources, and the temporal collocation window is 60 min for GDAS and QuikSCAT and 35 min for SSM/I. Before collocation, the eight retrieval cells along both edges of the QuikSCAT swath were removed, because they contain less than the optimal four beam combinations, and have degraded wind vectors [11].

The regression training dataset is quality controlled through exclusion of every condition listed in the next paragraph and SDRs that are likely influenced by thermal gradients in the warm load. No such exclusions are made in the testing dataset; instead, quality control flags are set during retrieval.

Retrievals are performed for all SDRs except those in the aft scan [1], with surface type other than ocean (no coast or near coast), with one or more  $T_B$  outside the physical bounds for no or light rain, or with any EIA outside the expected range (i.e., more than  $0.5^\circ$  from nominal). The following are flagged as “low confidence retrievals”: 1) in lakes or inland seas; 2) retrieval cell may contain rain; 3) in areas found to periodically suffer from radio-frequency interference (RFI) or ice contamination; and 4) are likely to suffer land contamination (within 105 km or 1.75 retrieval cell HPBW from nearest land). Condition (2) is determined using an SSMI-type rain flagging adapted to WindSat frequencies [13]. Static, geographical masks define the other conditions.

#### VI. RETRIEVAL PERFORMANCE

The retrieval performance in this section excludes low confidence retrievals, which are 20% of the total.<sup>1</sup> The Faraday rotation correction necessary to optimize  $\varphi$  retrieval performance is under validation, and has not been applied to the SDRs in the regression testing and training datasets.

Wind vector retrieval errors are computed relative to collocated QuikSCAT data (Section V). The QuikSCAT testing data has errors relative to *in situ* ground truth, as does the QuikSCAT and GDAS data used for wind vector regression training. However, the errors computed here should be good approximations (and likely upper bounds) to those that would be obtained by training and testing with actual ground truth data (or by training with  $T_B$  simulated using a physical model calibrated to ground truth, and testing with ground truth).

Table II shows the overall regression retrieval errors. Given the considerations above, the overall  $W$  rms error is well within 1.0 m/s. Training the  $W$  regression on a natural, nonuniform distribution of wind speeds (as contained in the collocated data) initially resulted in a large  $W$  bias error at high wind speeds ( $-4$  m/s at 23 m/s). We greatly reduced this bias (at the expense

<sup>1</sup>89% of low confidence retrievals were flagged for possible rain, 3% for RFI/ice, 10% for land contamination, and 1% for inland lakes and seas; multiple flags can be set for each retrieval. The rain flag was developed for filtering all rain cases from the training data, and therefore errs on the cautious side and overestimates the occurrence of rain.

TABLE II  
OVERALL RETRIEVAL ERRORS FOR REGRESSIONS

Retrieval (units)	$N_{\text{obs}}$ ( $\times 10^6$ )	Bias	Std. Dev.	RMS
$W$ (m/s)	20.8	-0.18	0.79	0.81
$U_1$ (m/s)	20.8	0.26	3.39	3.40
$U_2$ (m/s)	20.8	-0.02	2.47	2.47
$U_3$ (m/s)	20.8	0.02	3.70	3.70
$U_4$ (m/s)	20.8	-0.01	2.57	2.57

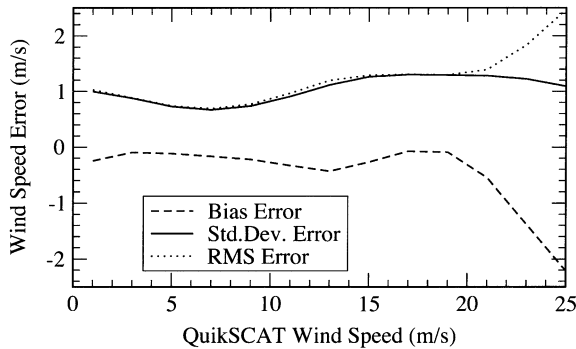


Fig. 1. WindSat wind speed errors stratified by QuikSCAT wind speed.

of introducing a small overall bias) by weighting each of the collocated observations in the regression training by the reciprocal of the square root of the wind speed distribution [14]. The stratification of the  $W$  retrieval errors versus the QuikSCAT wind speed is shown in Fig. 1.

The overall regression errors for  $U_1$  through  $U_4$  in Table II are much larger than those for  $W$ . This occurs because the wind speed signal in  $T_h$  is large [5], while the directional signals are relatively small [6], [15]. The  $U_1$  through  $U_4$  regressions must extract parts of the small directional signals, while compensating for atmospheric and SST variations. Because of the sine/cosine dependence of the wind direction signals, the  $U_1$  and  $U_3$  regressions use mainly  $T_v$  and  $T_h$ , while the  $U_2$  and  $U_4$  regressions use mainly  $T_v$  and  $T_4$ . Because the wind direction signals for  $T_v$  and  $T_h$  are superposed on a large and highly variable nondirectional component, the regression errors for  $U_1$  and  $U_3$  are larger than those for  $U_2$  and  $U_4$ .

Fig. 2 shows the wind direction rms errors for the first ranked (FR), median filtered (MF), median filtered with nudging (MFNG) ambiguities, and the closest ambiguity to the collocated wind direction (CL). The wind direction bias error at all  $W$  is small (less than  $3^\circ$ ) and is not shown.

Above 12 m/s, the agreement between the wind direction retrievals and QuikSCAT is excellent for all of the above ambiguities. Our initial wind direction performance is within  $20^\circ$  of QuikSCAT for wind speeds above 9.9, 8.8, 7.6, and 7.2 m/s for the FR, MF, MFNG, and CL ambiguities, respectively. Below 5 m/s, the wind direction signals are very small [6], [15], and the wind direction retrieval performance degrades accordingly.

Fig. 3 shows the skill (percentage of retrievals where the selected ambiguity is the CL ambiguity) for the FR, MF, and MFNG ambiguities, and the total number of ambiguities. Despite high FR skill, the median filter by itself makes only a small improvement in the wind direction error ( $6^\circ$  to  $8^\circ$  below 8 m/s, less than  $3^\circ$  above). One reason is that the number of

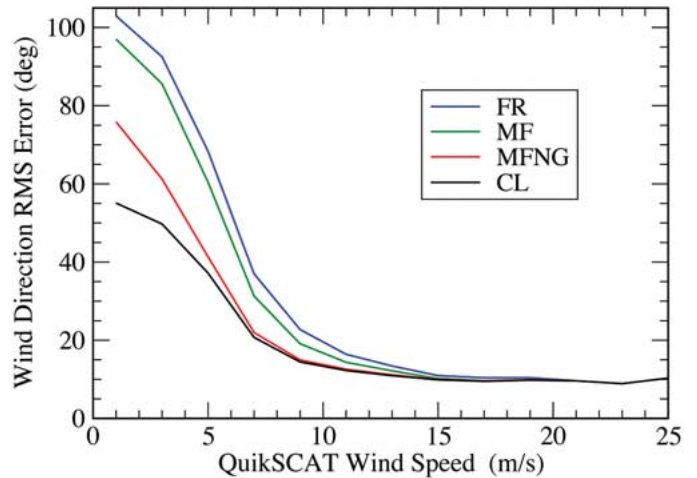


Fig. 2. WindSat wind direction rms errors stratified by QuikSCAT wind speed. Errors are determined relative to the collocated QuikSCAT science product.

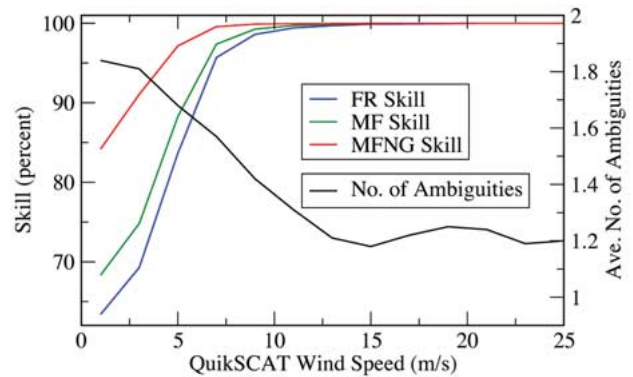


Fig. 3. Wind direction skill and mean number of ambiguities stratified by QuikSCAT wind speed.

ambiguities is low. Due to the requirement that the MLE-retrieved wind speed be nonnegative (Section III), there are no more than two ambiguities for any retrieval,<sup>2</sup> with an average of 1.56 over all retrievals. Thus, the median filter cannot improve 44% of the retrievals. Another reason is that, when one considers only retrievals with two ambiguities, the skill is reduced from that shown in the figure; for example the FR skill drops from 84% to 76% at 5 m/s.

Additionally, MF wind fields show good qualitative agreement with QuikSCAT wind fields except inside some regions where  $W < 6$  m/s and wind direction is changing rapidly; there, low-skill degraded retrievals often occur in contiguous patches. By itself, the median filter rarely improves upon the FR ambiguity in such patches. Analogous to scatterometer retrievals, we have found that the separation between the first and second rank ambiguities is about  $180^\circ$ , which may further inhibit median filter performance in and near the patches. Nudging, which can select the second rank ambiguity to initialize the median

<sup>2</sup>Without this requirement, the maximum number of ambiguities is 3. However, ambiguities with negative  $W_{\text{min}}$  always have the highest chi-square of any ambiguity (often by an order of magnitude), have a value near  $-1$  m/s, regardless of the magnitude of the wind speeds computed from  $(U_1, U_2)$  and  $(U_3, U_4)$  vectors, and appear when these two wind speeds are grossly inconsistent. Thus, we consider ambiguities with negative  $W_{\text{min}}$  to be an unphysical result obtained when the MLE is given inconsistent values of  $U_1$  through  $U_4$ . As such, they should be discarded.

filter, allows significant improvement in the agreement between MFNG and QuikSCAT wind fields over the patches, and thus in wind direction performance at low and intermediate wind speeds.

Because nudging chooses between two ambiguities separated by approximately  $180^\circ$ , small to moderate perturbations to the wind field used for nudging will have little effect on the nudged wind field used to initialize the median filter [11]. Therefore, the incorporation of QuikSCAT data into GDAS wind fields should not significantly affect the nudged wind field, or the comparison of the MFNG ambiguities with QuikSCAT.

## VII. CONCLUSION

We have developed a regression retrieval technique for WindSat retrieval of ocean surface wind speed and a combination regression/MLE technique for ocean surface wind direction retrieval. The regressions were derived empirically, using collocated NWP data and satellite-based retrievals. Together, they provide an initial assessment of WindSat retrieval capabilities. Comparisons of the initial WindSat retrievals with QuikSCAT wind vectors have demonstrated the capability for passive microwave wind direction retrieval, and show excellent agreement with QuikSCAT wind speeds.

We expect the retrievals to improve due to ongoing work on the SDR algorithm, quality control flagging, and the retrieval algorithms. Ongoing work on the SDR algorithm includes addition of corrections for Faraday rotation and thermal gradients in the warm calibration load. We are also working on improved rain flagging, and replacement of the sea ice and RFI geographical masks with dynamic ice and RFI detection. Retrieval algorithm work includes using nonuniform bin widths in the second-stage regressions, tuning the median filter, and incorporating buoy observations into the regression training and testing.

## ACKNOWLEDGMENT

The authors would like to thank L. Connor for his work in assembling the collocated datasets, S. Cox for performing the error analysis, and P. Crane for assisting in initial development of the regression software.

## REFERENCES

- [1] P. W. Gaiser, K. St. Germain, E. M. Twarog, G. A. Poe, W. Purdy, D. Richardson, W. Grossman, W. L. Jones, D. Spencer, G. Golba, M. Mook, J. Cleveland, L. Choy, R. M. Bevilacqua, and P. Chang, "The WindSat spaceborne polarimetric microwave radiometer: Sensor description and early orbit performance," *IEEE Trans. Geosci. Remote Sens.*, vol. 42, no. 11, pp. 2347–2361, Nov. 2004.
- [2] W. E. Purdy, P. W. Gaiser, G. A. Poe, E. A. Uliana, T. Meissner, and F. Wentz, "Geolocation and pointing accuracy analysis for the WindSat sensor," *IEEE Trans. Geosci. Remote Sens.*, vol. 44, no. 3, Mar. 2006, to be published.
- [3] D. B. Kunke, N. S. Chauhan, and J. J. Jewel, "Phase one development of the NPOESS Conical-Scanning Microwave Imager/Sounder (CMIS)," in *Proc. IGARSS*, vol. 2, Toronto, ON, Canada, Jun. 24–28, 2002, pp. 1005–1007.
- [4] T. T. Wilheit and A. T. C. Chang, "An algorithm for retrieval of ocean surface and atmospheric parameters from the observations of the Scanning Multichannel Microwave Radiometer," *Radio Sci.*, vol. 15, no. 3, pp. 525–544, May–Jun. 1980.
- [5] F. J. Wentz and T. Meissner, "AMSR Ocean Algorithm, Version 2," Remote Sensing Systems, Santa Rosa, CA, Algorithm Theoretical Basis Document, Tech. Rep. 121599A, Nov. 2000.
- [6] S. H. Yueh, W. J. Wilson, S. J. Dinardo, and F. K. Li, "Polarimetric microwave signatures of ocean wind directions," *IEEE Trans. Geosci. Remote Sens.*, vol. 37, no. 2, pp. 949–959, Mar. 1999.
- [7] S. H. Yueh, R. Kwok, and S. V. Nghiem, "Polarimetric scattering and emission properties of targets with reflection symmetry," *Radio Sci.*, vol. 29, no. 6, pp. 1409–1420, Nov./Dec. 1994.
- [8] F. J. Wentz, "A well-calibrated ocean algorithm for the Special Sensor Microwave/Imager," *J. Geophys. Res.*, vol. 102, no. C4, pp. 8703–8718, Apr. 1997.
- [9] C. D. Rodgers, *Inverse Methods for Atmospheric Sounding: Theory and Practice*. Singapore: World Scientific, 2000, pp. 20–25, 32, 66, 84.
- [10] S. J. Shaffer, R. S. Dunbar, S. V. Hsiao, and D. G. Long, "A median-filter-based ambiguity removal algorithm for NSCAT," *IEEE Trans. Geosci. Remote Sens.*, vol. 29, no. 1, pp. 167–174, Jan. 1991.
- [11] B. W. Stiles, B. D. Pollard, and R. S. Dunbar, "Direction interval retrieval with threshold nudging: A method for improving the accuracy of QuikSCAT winds," *IEEE Trans. Geosci. Remote Sens.*, vol. 40, no. 1, pp. 79–89, Jan. 2002.
- [12] E. Twarog, P. W. Gaiser, B. Purdy, L. Jones, K. St. Germain, and G. Poe, "WindSat post-launch calibration," in *Proc. IGARSS*, Anchorage, AK, 2004, pp. 375–378.
- [13] M. H. Bettenhausen, C. K. Smith, R. M. Bevilacqua, N.-Y. Wang, P. W. Gaiser, and S. Cox, "A nonlinear optimization algorithm for WindSat wind vector retrievals," *IEEE Trans. Geosci. Remote Sens.*, vol. 44, 2006, to be published.
- [14] L. N. Connor and P. S. Chang, "Ocean surface wind retrievals using the TRMM Microwave Imager," *IEEE Trans. Geosci. Remote Sens.*, vol. 38, no. 4, pp. 2009–2016, Jul. 2000.
- [15] T. Meissner and F. Wentz, "An updated analysis of the ocean surface wind direction signal in passive microwave brightness temperatures," *IEEE Trans. Geosci. Remote Sens.*, vol. 40, no. 6, pp. 1230–1240, Jun. 2002.